REPORT DOCUMENTATION PAGE

Form Approved
OMB No. 0704-0188

1. AGENCY USE ONLY *(Leave blank)*	2. REPORT DATE	3. REPORT TYPE AND DATES COVERED
	June 2007	Final Progress Report

4. TITLE AND SUBTITLE
Plasmon Resonators for Quantum Computing

5. FUNDING NUMBERS
FA9550-04-1-0247

6. AUTHORS
Dr. Philip Hemmer

7. PERFORMING ORGANIZATION NAME(S) AND ADDRESS(ES)
Texas Engineering Experiment Station (TEES)
332 Wisenbaker Bldg. MS 3000
College Station, Texas 77843-3000

8. PERFORMING ORGANIZATION REPORT NUMBER

9. SPONSORING/MONITORING AGENCY NAME(S) AND ADDRESS(ES)
Air Force Office of Scientific Research

10. SPONSORING/MONITORING AGENCY REPORT NUMBER
AFRL-SR-AR-TR-07-0487

11. SUPPLEMENTARY NOTES

12a. DISTRIBUTION/AVAILABILITY STATEMENT
Unlimited

12b. DISTRIBUTION CODE
UL

13. ABSTRACT *(Maximum 200 words)*

The purpose of this project was to develop high-performance plasmon-based nano-optics that can be used to coherently couple single optical emitters to each other or to incoming photons for quantum information applications. The constraint was to fabricate these structures with nanolithographic process such as e-beam lithography, so that precise reproducibility and placement accuracy can be achieved. Initially, the emphasis was on duplicating the performance of fractal-like structures grown by self-assembly. However, difficulties in achieving the necessary sub-5-nm resolution led to the exploration of two other structures. One of these was an infrared LC resonator with an adjustable coupling to the IR field. The motivation for this was to allow optimization of the structure so that an optical version it could be placed on a high Q evanescent optical cavity, without degrading cavity performance. A microwave-frequency version of the structure was first fabricated and tested with a custom near-field probe to validate the simulations. The second structures to be studied were optical wires with normal incidence input/output light coupling structures. Wires with dimensions as low as 50 x 50 nm with lengths up to 15 microns were fabricated. The transmission losses at 632 nm compared favorably to self-assembled metal wires.

14. SUBJECT TERMS
quantum computing, nano-optics, plasmon

15. NUMBER OF PAGES
19

16. PRICE CODE

17. SECURITY CLASSIFICATION OF REPORT	18. SECURITY CLASSIFICATION OF THIS PAGE	19. SECURITY CLASSIFICATION OF ABSTRACT	20. LIMITATION OF ABSTRACT
UNCLASSIFIED	UNCLASSIFIED	UNCLASSIFIED	SAR (same as report)

DTIC Data

Purchase Request Number: FQ8671-0600487

BPN: F1ATA05258B487

Proposal Number: 04-NE-095

Research Title: (THEME 2 QUANTUM COMPUTING) PLASMON RESONATORS FOR QUANTUM COMPUTING

Type Submission: Final Report

Inst. Control Number: FA9550-04-1-0247P00002

Institution: TEXAS ENGINEERING EXPERIMENT STATION

Primary Investigator: Dr. Philip R. Hemmer

Invention Ind: none

Project/Task: 2305D / X

Program Manager: Gernot S. Pomrenke

Objective:

The objective is to investigate plasmon resonators for scalable quantum computing and related applications. For solid-state quantum computing and spin-off applications, it is essential to have strong coupling between the electromagnetic field and a single atom, molecule, or quantum dot. Ordinarily this strong coupling is achieved using high Q optical resonators. The goal is to develop high-performance plasmon-resonator enhanced optical cavities that can be reproduced using nanolithography. Ideally these will perform as well as the best fractal enhanced cavities fabricated by the nanosphere accretion technique.

Approach:

Nano-scale sub-wavelength plasmon resonators will be fabricated by e-beam lithography, and evaluated to determine their suitability for solid-state quantum computing and other applications. This will include the fabrication of metallic fractal patterns, whose performance can be directly compared to fractal patterns generated by the conventional metal ball accretion technique. Emphasis will be on reproducibility of particular plasmon resonators with regard to their optical properties, and quantifying the ability of these plasmon structures to enhance the performance of optical cavities, or example photon band gap (PBG) cavities. Plasmon resonators operating at visible wavelengths are preferred, but in the initial stages infrared and even microwave versions will be investigated to relax the tolerances of the nanofabrication process.

Progress:

Year: 2005 **Month:** 10

Subwavelength microwave resonators based on double-ridge waveguides are proposed for applications that require strong electromagnetic fields under the constraint of limited microwave power. A key advantage of the proposed resonator structure is that magnetic couplings to the environment can be precisely controlled over a wide range of values with minimal impact on the resonance frequencies and quality factors. Another advantage is that inductances and capacitances are independent of each other, which offers flexibility in resonator design. A theoretical analysis for resonant conditions is given, and both numerical simulations and experimental measurements confirm that the resonators enhance electromagnetic fields by a factor of 40 in the near-field, equivalent to an effective electromagnetic energy density increase of 1600. The resonators are electrically small in size, have a high quality factor, and are suitable for the research of microwave frequency quantum electrodynamics.

Year: 2006 **Month:** 10

A key advantage of the proposed resonator structure is that magnetic couplings to the environment can be precisely controlled over a wide range of values with minimal impact on the resonance frequencies and quality factors. Another

DTIC Data

Progress:

Year: 2006 **Month:** 10

advantage is that inductances and capacitances are independent of each other, which offers flexibility in resonator design. A theoretical analysis for resonant conditions is given, and both numerical simulations and experimental measurements confirm that the resonators enhance electromagnetic fields by a factor of 40 in the near-field, equivalent to an effective electromagnetic energy density increase of 1600. The resonators are electrically small in size, have a high quality factor, and are suitable for the research of microwave frequency quantum electrodynamics. Subwavelength microwave resonators based on double-ridge waveguides are proposed for applications that require strong electromagnetic fields under the constraint of limited microwave power.

Year: 2006 **Month:** 12

Summary:
The purpose of this project is to develop high-performance plasmon-resonator enhanced optical cavities that can be reproduced using nanolithography. Ideally these will perform as well as the best fractal enhanced cavities fabricated by the nanosphere accretion technique. The devices will then be evaluated for suitability for quantum computing applications, as well as spin-off applications such as sensitive chemical-biological detection, and possibly quantum dot detectors. An additional goal will be to develop infrared and microwave versions of plasmon resonators that can be investigated for potential spin-off applications in these frequency ranges.

Progress has been rapid in the past year. We have fabricated optical wires operating near the target wavelength of 637 nm with much lower losses than predicted by theory, namely ~0.1 dB/micron. We have also inferred an out-coupling efficiency >30%, which is high enough for many quantum information applications. The in-coupling efficiency is still low but preliminary data on new coupling structures suggests that it may be possible to increase significantly using structures such as bow-tie antennas in place of our grating couplers. We have asked for a no-cost extension to give us time to complete the analysis of these encouraging results.

Year: 2007 **Month:** 09 **Final**

The purpose of this project was to develop high-performance plasmon-based nano-optics that can be used to coherently couple single optical emitters to each other or to incoming photons for quantum information applications. The constraint was to fabricate these structures with nanolithographic process such as e-beam lithography, so that precise reproducibility and placement accuracy can be achieved. Initially, the emphasis was on duplicating the performance of fractal-like structures grown by self-assembly. However, difficulties in achieving the necessary sub-5-nm resolution led to the exploration of two other structures. One of these was an infrared LC resonator with an adjustable coupling to the JR field. The motivation for this was to allow optimization of the structure so that an optical version it could be placed on a high Q evanescent optical cavity, without degrading cavity performance. A microwave-frequency version of the structure was first fabricated and tested with a custom near-field probe to validate the simulations. The second structures to be studied were optical wires with normal incidence input/output light coupling structures. Wires with dimensions as low as 50 x 50 nm with lengths up to 15 microns were fabricated. The transmission losses at 632 nm compared favorably to self-assembled metal wires.

Final report, FA9550-04-1-0247

Plasmon Resonators for Quantum Computing

Executive summary:

The purpose of this project was to develop high-performance plasmon-based nano-optics that can be used to coherently couple single emitters, such as nitrogen-vacancy (NV) color centers in diamond, to each other or to photons for quantum information applications. The constraint is to fabricate these structures with nano-lithographic process such as e-beam lithography, so that precise reproducibility and placement accuracy can be achieved. This is essential for manufacturability, as well as chip-level integration with other devices. The goal was to achieve the same performance with lithographically fabricated devices as has already been demonstrated for self-assembled devices. Ideally these plasmon devices should be compatible with high Q optical micro-cavities so as not to spoil their Q, thereby achieving multiplicative enhancement, for example as in fractal-enhanced cavities. Aside from quantum computing applications, there will be many spin-off applications such as sensitive chemical-biological detections, high-temperature infrared photo-detectors, and possibly novel multi-spectral detectors.

Initially, the emphasis was on duplicating the performance of fractal-like structures grown by self-assembly. However, difficulties in achieving the necessary sub-5-nm resolution led to the exploration of two other structures. One of these was an infrared LC resonator with an adjustable coupling to the IR field. The motivation for this was to allow optimization of the structure so that it could be placed on a high Q evanescent optical cavity, without degrading cavity performance. A microwave-frequency version of the structure was first fabricated and tested with a custom near-field probe to validate the simulations. Variable coupling with minimal change in Q and center frequency were successfully demonstrated. An infrared version was then fabricated and tested. However, the resolution limit of the FTIR microscope used to characterize it, led to a high background light level that prevented conclusive analysis.

The second structures to be studied were optical wires with normal incidence input/output light coupling structures. Originally, these were intended to be test structures that would be used to characterize other devices such as the LC resonators. By confining light to propagate along a wire in a highly spatially confined mode, other small devices could be easily tested without the problem of background light. Surprisingly, theoretical estimates revealed that these optical wires alone could achieve enough field confinement to enable the intended quantum information applications. Fabrication of the wires was also highly successful. Wires with dimensions as low as 50 x 50 nm with lengths up to 15 microns were fabricated. Surprisingly the transmission losses, between 0.1 and 0.5 dB/micron at 632 nm, compared favorably to self-assembled metal wires, even though the nano-fabricated wires were not single crystals. Indirect evidence of strong optical confinement was also observed. The coupling structures were found to have efficiencies in the range of fractional percent for input and 35% for output.

1. Relation to quantum computing:

For solid-state quantum computing and communication it is essential to have strong coupling between the electromagnetic field and a single atom, molecule, or quantum dot. For free atoms this strong coupling is achieved using high Q optical resonators, such as ultra-low-loss bulk Fabry-Perot cavities or whispering gallery modes of micro-sphere optical cavities, which have Q values well in excess of 10^7. Unfortunately, such high Q values are not achieveable for every material system, for example in the case of nitrogen-vacancy (NV) diamond it is possible to construct relatively high Q optical micro-disk cavities with thin films, but NVs in these thin films do not have good optical spectral stability. Conversely, stable NVs are found in ultra-pure single crystal diamonds but these can not be easily made into high Q micro-cavities. To solve this problem, hybrid resonators consisting of both a conventional optical cavity and a plasmon resonator can be used to multiplicatively enhance the local field and therefore dramatically increase the vacuum Rabi frequency. If this is done without the plasmon structures introducing loss into the optical cavity, then the quantum fidelity can be high enough for quantum information/computing applications.

Thus far, plasmon resonators based on fractals have been shown to localize optical fields to "hot spot" sizes of 50 nm or less. This effectively focuses the field, giving a very large vacuum Rabi frequency. More importantly, these structures do not appear to significantly shorten the photon lifetime. This is based on the observation that metal fractal patterns, when placed on high Q whispering gallery mode cavities, give multiplicative Q values. In fact, combined Q values in excess of 10^{10} have been observed. Since these fractal patterns can be deposited on most surfaces, they are compatible with a large class of solid state materials and cavity designs, such as PBG.

To make such plasmon resonators manufacturable, scalable, and applicable to solid state quantum computer arrays, they must be fabricated using nano-lithography. Metallic nanostructures fabricated in this way would have known, reproducible properties and be placed in well-defined locations, as required for chip integration.

2. Self-assembled fractal-like plasmon resonators.

Currently, the highest-performance plasmon nano-optic devices are produced by chemical self-assembly techniques. For example, in the case of fractal-based plasmon nano-optics the devices are fabricated by cluster-cluster aggregation of monomer particles, formed by the addition of an organic acid to an aqueous solution of metal nanoparticles with average diameters on the order of 25 nm.[1] The metallic patterns are subsequently adsorbed on the surface of a dielectric substrate in contact with the solution. The resulting metallic structures occasionally exhibit optical intensity enhancement up to 4 – 5 orders of magnitude. In fact, when deposited on high Q evanescent cavities, the effects can be multiplicative producing giant field enhancement. For example, these structures have shown Raman enhancement on the order of 10^{15} or more, where the field amplification so large that high-order Raman and hyper-Raman resonances are as strong, or stronger than, linear absorption, even when excited with low power cw lasers.

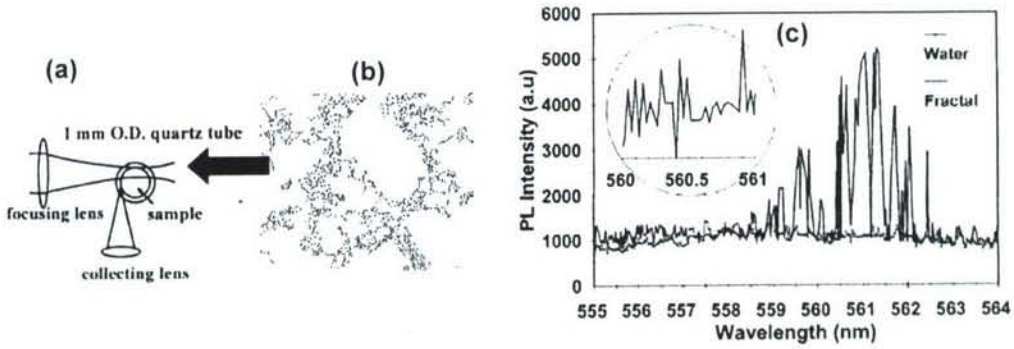

Figure 1. (a) Excitation of a high Q whispering gallery mode on a cylindrical glass cavity. (b) Fractal-like metal plasmon nanostructures grown on the glass cavity surface. (c) Evidence of strong local field enhancement due to both fractals and cavity combined.

The problem with the self-assembly fabrication process is that it is inherently probabilistic. Although optimum structures are routinely produced at many locations on a substrate, no two are exactly alike. Hence there is no way to exactly reproduce a specific pattern, much less with its hot spot located at a pre-determined position, as required for chip-level sensor integration.

To solve the reproducibility problem of chemical self-assembly, one can envision using nano-lithography. However, the resolution required to duplicate the self-assembled nano-optic structures is on the scale of 5 nm or less, and this pushes the limits of current state-of-the-art nano-lithography. While individual elements on this size scale have been fabricated using e-beam lithography, the reproducibility is poor and attempts to locate many such features in close proximity inevitably leads to over-exposure and bridging of elements.

We have attempted e-beam lithography combined with both metal deposition and etching, as well as focused ion beam (FIB) fabricated structures, but have not been able to achieve reproducible patterns with feature sizes below ~30 nm.

---

[1] "Fractals in microcavities: giant coupled, multiplicative enhancement of optical response," W. Kim, V.P. Safonov, V.M. Shalaev, and R.L. Armstrong, *Phys. Rev. Lett.* **82**, pg. 4811 (1999).

3. Infrared LC resonators with variable coupling.

Due to the difficulty of fabricating metallic patterns with feature sizes of less than 5 nm, which are needed to reproduce self-assembled fractal patterns, we began looking at longer wavelength structures. In the infrared region, the wavelengths are a factor of 10 larger than the optical wavelength, so that we only need 50 nm feature sizes. This can easily be reached with standard e-beam lithography. From the applications point of view, there are also advantages to working in this wavelength range, for example many Air Force sensors prefer this wavelength range. Therefore the potential for spin-off applications is actually higher than in the visible.

In the IR, we concentrated on LC plasmon resonators. With the eventual goal of incorporating these onto an optical cavity structure, emphasis was placed on developing structures with variable coupling. The motivation for this was to allow optimization of the structure so that it could be placed on a high Q evanescent optical cavity, without degrading cavity performance. Too strong coupling to the optical cavity mode will result in losses that reduce the cavity Q and degrade the field strength. Too weak coupling to the cavity will prevent the plasmon structure from further enhancing the field strength. Consequently we must control coupling between plasmon and cavity modes in a way that is independent of structure size, so that it can be made as small as possible to further reduce losses and enhance confinement. By adjusting the coupling of such a structure it should be possible to achieve the goal of multiplicative field enhancement.

To begin with, a microwave-frequency version a LC resonator with adjustable coupling was designed first. This motivation was that no such structures had been attempted before and it was easier to validate the theory in the microwave range. In the microwave region, it is also easy to fabricate complex sub-wavelength structures, even without e-beam lithography. Using microwave simulation tools, we quickly evaluated a number of structures and chose the one shown in Figure 2.

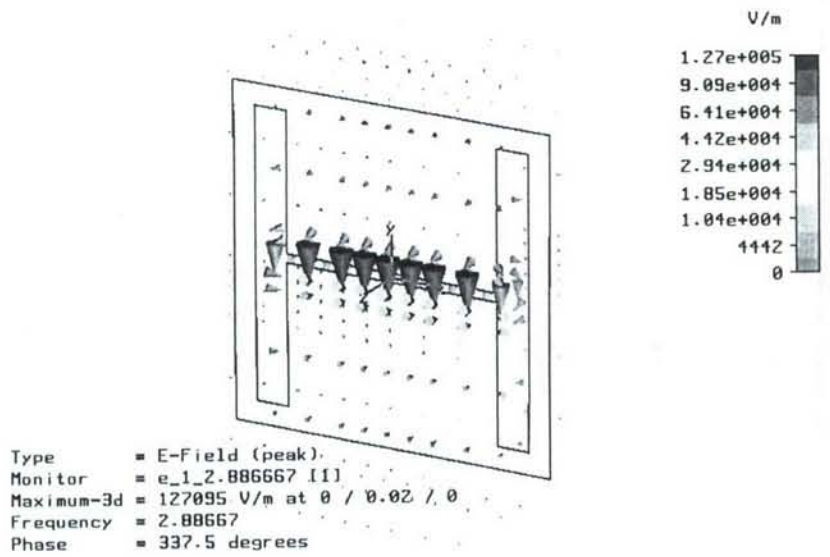

Figure 2. Split ring resonator structure showing the electric field distribution on resonance.

This sub-wavelength split-ring resonator has variable coupling to the magnetic field of the microwaves. When the loops are equal size, a normal magnetic field induces equal but opposite currents in the central capacitor. The net result is zero electric field at the central gap and so there is no coupling to the dominant resonator mode. Due to the small size of the capacitor gap, E-field coupling is minimal. When the loops are made different sizes (asymmetric), the coupling goes from near zero to strong, as verified by the amount of stored power in the LC resonator. In Figure 3 we show a simulation of this stored power as a function of asymmetry of the structure while keeping the outer dimensions constant. Clearly, we are able to control the coupling over a wide range, as required.

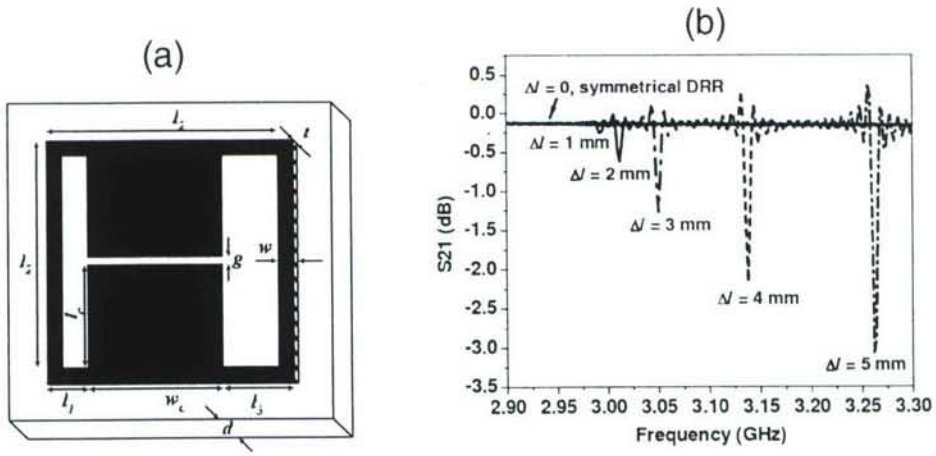

Figure 3. (a) Asymmetric split ring resonator. (b) Resonator stored power vs asymmetry.

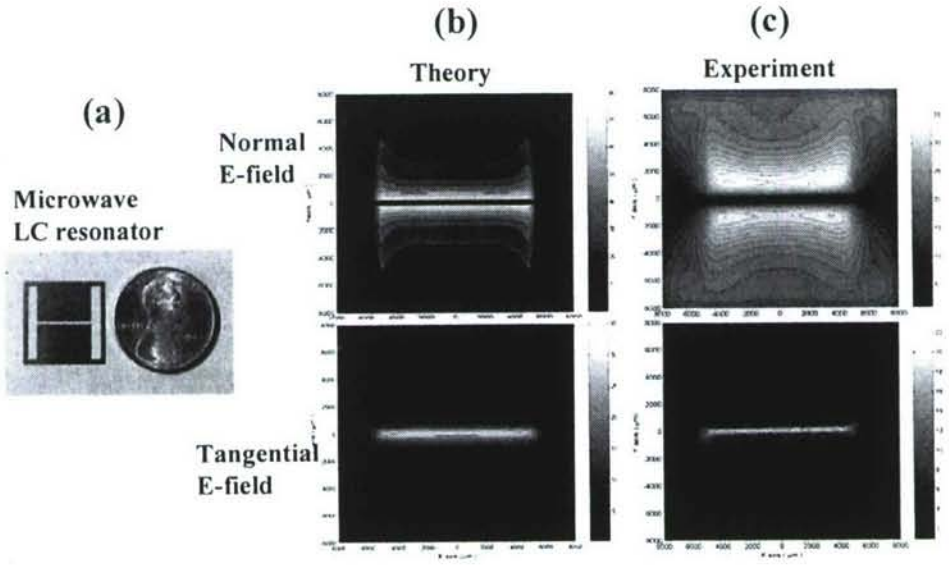

Figure 4. (a) Fabricated microwave split ring resonator. (b) Simulation of the resonator showing near field enhancement of the electric field in both normal (to fabrication surface) and tangential components. (c) Measured near field enhancement of normal and tangential electric field components.

We simulated, fabricate and tested these split ring resonators to quantify the field enhancement. The results are shown in Figure 4. To measure the microwave near field enhancement we built a high resolution microwave near field probe. This microwave probe consisted of a small wire oriented either normal or parallel to the surface depending on measured field direction. As shown the agreement between theory and experiment is good.

In parallel with the microwave optimization experiments, we are designing infrared structures to test the ability of the microwave simulation tool to accurately predict the observations in this region. To this end, Figure 5 shows microwave and infrared split ring resonators side by side. As shown, the infrared resonator dimensions are approximately 5000 times smaller than the microwave device. A comparison of the predicted LC resonance frequencies for these two structures are shown in Figure 6. Here, the field enhancements are plotted as a function of frequency. As seen, the LC resonance frequency scales approximately with device size in going from microwave to infrared. The infrared resonance is at a wavelength of about 7 microns, which is chosen because it is the region of maximum sensitivity of our infrared FTIR microscope. Note that although the field enhancement, compared to that of the incident plane wave, is smaller for the infrared structure, it is still 100,000 times.

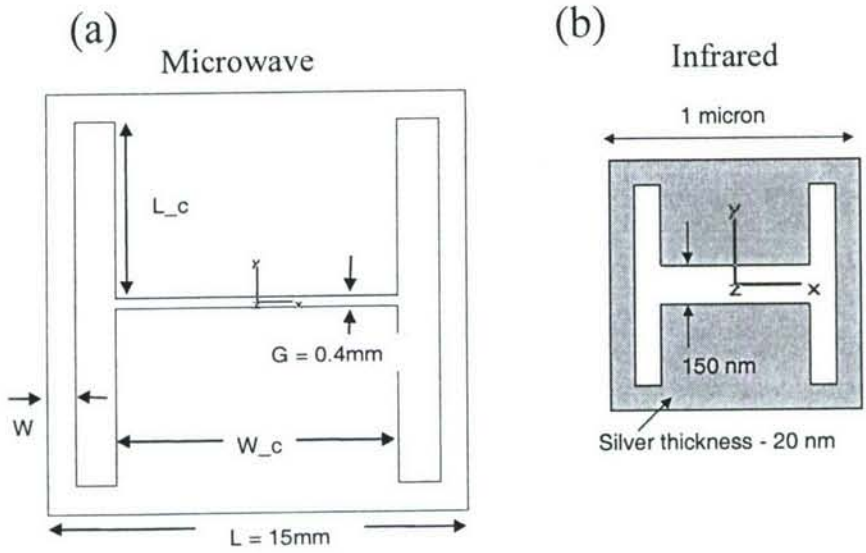

Figure 5. (a) Original microwave split ring resonator showing dimensions. (b) Infrared version of the split ring resonator and its dimensions.

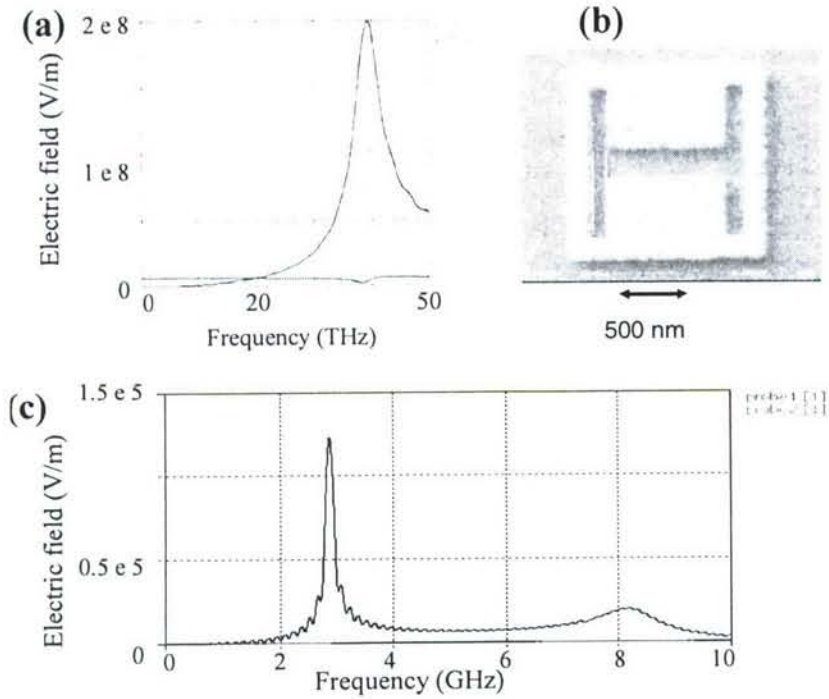

Figure 6. (a) Simulation of the infrared electric field enhancement due to LC resonance in the infrared structure of Figure 5. (b) Silver IR resonator, 20 nm thick. (c) The electric field enhancement of the corresponding microwave structure, shown for comparison.

4. Optical nano-wires.

Originally, we explored nano-wires as test structures that would be used to characterize other devices such as the LC resonators. By confining light to propagate along a wire in a highly spatially confined mode, other plasmon nano-optic devices could be easily tested without the problem of background light. Surprisingly, theoretical estimates revealed that these optical wires alone could achieve enough field confinement to enable the intended quantum information applications. These calculations are summarized in Figure 7. Here Figure 7(a) shows the model of surface plasmons as electromagnetic excitations associated with charge density waves on the surface of a conducting object.

Figure 7(b) shows the model for plasmons on a cylindrical nano-wire. This problem can be solved exactly and the solutions are shown in Figure 7(c) for several modes as a function of wire radius. As can be seen, all but the lowest order modes are cut off ($k\| = 0$) as the wire radius shrinks. However the lowest order mode survives and becomes extremely confined. Typical transverse confinement is on the order of the nano-wire radius. There is also lateral confinement in the sense that the plasmon propagation wavelength shrinks ($k\|$ diverges) which also means that the phase velocity goes to zero (see Figure 7(d)).

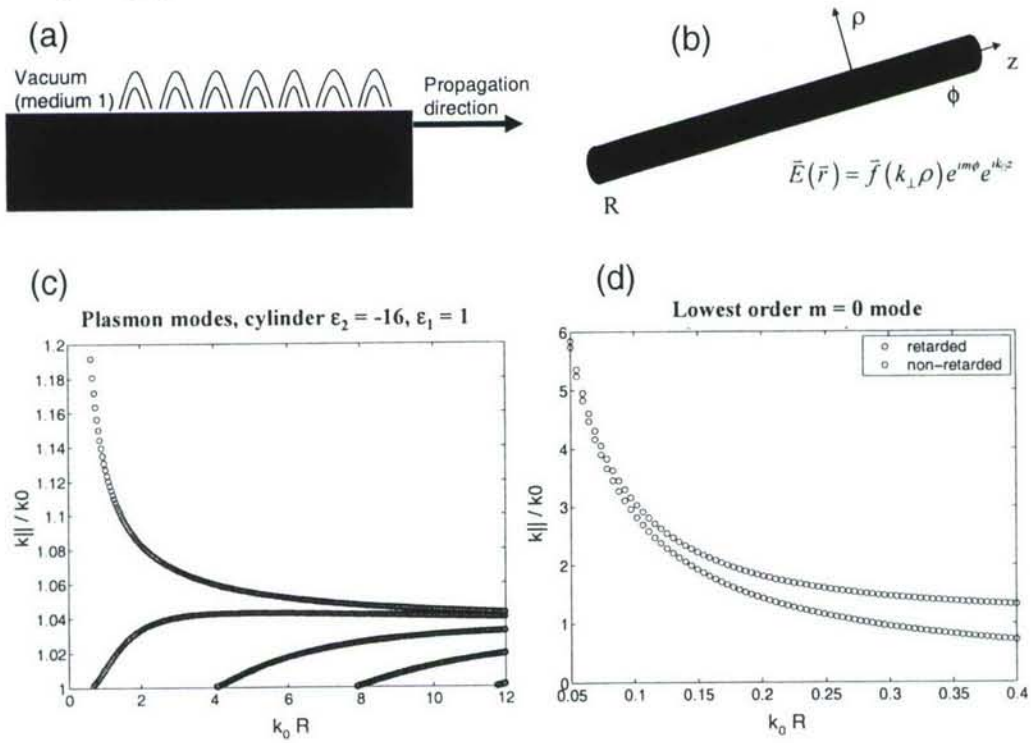

Figure 7. (a) Plasmons on a metal boundary can be viewed as charge density waves that propagate along the surface, dragging along an electromagnetic field. Their wavelength is shorter than that in free-space and so they cannot couple directly to radiating modes. (b) Surface modes can exist around a cylindrical metal wire. (c) As the wire radius is reduced one mode becomes strongly localized, k_0 R >> 1. (d) As the mode becomes more localized, its wavelength gets shorter.

As the nanowire radius shrinks, and the confined mode is concentrated there can be enhanced coupling to a single emitter, such as an atom or single NV diamond color center. Figure 8 shows the efficiency for extraction of a single photon from a single excited atom as a function of nano-wire radius. In Figure 8(a) the atom emits into the nano-wire and is then coupled into the optical waveguide. In Figure 8(b) the atom first emits into a sharp tip, then propagates down the nano-wire and into the waveguide. As can be seen in Figure 8(c), >70% photon collection efficiency is observed for a wire of radius ~1/5 of the optical wavelength. By placing the atom at the sharpened tip of a nano-wire, the out-coupling efficiency increases to 90%. Note that these estimates include optical radiation to free space as well as power absorbed by the metal in the nano-wire.

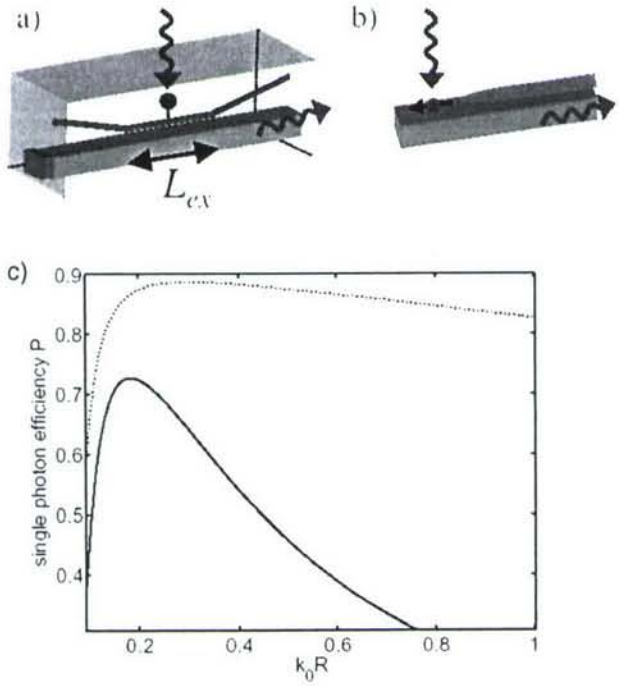

Figure 8. (a) Coupling of the emission of a single atom to an optical waveguide via a metal nano-wire. (b) Coupling of single-atom emission to a waveguide using a metal nano-wire with a sharp tip. (c) Efficiency for coupling emission from a single atom into an optical waveguide as a function of nano-wire radius, where k_0 is the optical wavelength in the absence of the wire. Since the efficiency depends on distance from the wire, the maximum efficiency is plotted. The solid curve is for an atom near a long nano-wire as in a). The dashed curve is for an atom near the sharpened tip of a nano-wire as in b).

The sub-wavelength waveguiding of plasmons in metallic nanowires has been observed in a number of recent experiments. These are summarized in Table 1. As shown, the reported propagation lengths do not exceed two microns so far for subwavelength waveguides in the visible spectrum. In this case, the waveguide width was 250 nm, or about half of the wavelength. However, the propagation length is much longer in the infrared (IR) region. As the wavelength goes up, the field is more displaced into the low-loss dielectric cladding rather than the lossy metal. Extremely long travel range was reported with a strip that has a width five times the telecommunication wavelength used.

As seen in Table 1, it is commonplace to use techniques such as end-fire coupling to fibers, but this becomes more difficult as the SP mode size shrinks in the visible. Here we note that special coupling techniques have been used in some cases, such as hole/dot array condensors and apertures.

Table 1. Summary of recent research on surface plasmon waveguides

Size (microns)	Range (microns)	Wavelength (nm)	Comments
8 x 0.02	1000	1550	Simulated by method of lines. Made by photolithography. End-fire coupled to fibers. Poor localization.[2]
1 x 0.07	< 10	633	No rigorous calculation. Asymmetric cladding. Made by photolithography or EBL. Prism coupled[3]
0.09 x 0.03 x 0.03 chain	0.2	633	Simulation by FDTD. Asymmetric cladding. Made by EBL.Excited by NSOM[4]
0.2 x 0.05	2.5	800	No rigorous calculation. Asymmetric cladding. Made by EBL. Prism coupled to tapered strip.[5]
0.6 x 1 V-groove	90 -- 250	1500	Calculation by effective index method. V groove No cladding. Made by focused ion beam. End-fire coupled to fibers.[6]

[2] [58] R. Charbonneau, P. Berini, E. Berolo, and E. Lisicka-Shrzek, "Experimental observation of plasmon polariton waves supported by a thin metal film of finite width," *Optics Letters*, vol. 25, pp. 844{846, 2000.;P. Berini, "Plasmon-polariton waves guided by thin lossy metal films of finite width: Bounded modes of symmetric structures," *Physical Review B*, vol. 61, pp. 10484{10503, 2000; P. Berini, R. Charbonneau, N. Lahoud, and G. Mattiussi, "Characterization of long-range surface-plasmon-polariton waveguides," *Journal of Applied Physics*, 100 vol. 98, pp. 043109, 2005.

[3] B. Lamprecht, J. R. Krenn, G. Schider, H. Ditlbacher, M. Salerno, N. Felidj, A. Leitner, and F. R. Aussenegg, "Surface plasmon propagation in microscale metal stripes," *Applied Physics Letters*, vol. 79, pp. 51, 2001.; J.-C. Weeber, J. R. Krenn, A. Dereux, B. Lamprecht, Y. Lacroute, and J. P. Goudonnet, "Near-field observation of surface plasmon polariton propagation on thin metal stripes," *Physical Review B*, vol. 64, pp. 045411, 2001.

[4] S. A. Maier, P. G. Kik, H. A. Atwater, S. Meltzer, E. Harel, B. E. Koel, and A. A.G. Requicha, "Local detection of electromagnetic energy transport below the diffraction limit in metal nanoparticle plasmon waveguides," *Nature Materials*, vol. 2, pp. 229{232, 2003; S. A. Maier, P. G. Kik, and H. A. Atwater, "Observation of coupled plasmon-polariton modes in Au nanoparticle chain waveguides of different lengths: Estimation of waveguide loss," *Applied Physics Letters*, vol. 81, pp. 1714, 2002

[5] J. R. Krennl and J.-C. Weeber, "Surface plasmon polaritons in metal stripes and wires," *Phylosophical Transactions of the Royal Society A*, vol. 362, pp. 739{756, 2004.; J. R. Krenn, B. Lamprecht, H. Ditlbacher, G. Schider, M. Salerno, A. Leitner, and F. R. Aussenegg, "Nondiffraction-limited light transport by gold nanowires," *Europhysics Letters*, vol. 60, pp. 663{669, 2002.

[6] S. I. Bozhevolnyi, V. S. Volkov, E. Devaux, and T. W. Ebbesen, "Channel plasmon-polariton guiding by subwavelength metal grooves," *Physical Review Letters*, vol. 95, pp. 046802, 2005.101

0.73 x 1 wedge	1.5, 2.25	633	Simulation by FDTD. No cladding. Made by focused ion beam. Coupled to in-plane apertures[7]
6.2 x 0.3	50, 320	1600	Simulation by FDTD. Si/Au/air. Made by lithography. Excited as a whole by a tapered fiber in parallel.[8]
0.23 x 0.12 dot chain	4	785	Simulation by FDTD. Made by focused ion beam. Excited at the focus of a SP condenser.[9]
0.25 x 0.05	2.0	532	Calculation with dipole models. Made by focused ion beam. Excited at the focus of a SP condenser.[10]
0.02	NA	532, 820	No rigorous calculation. Made by template-directed electrosynthesis. Excited by a total internal reflection prism[11]

The first plasmon nano-wire and coupling structures that were fabricated are simulated in Figure 9. As seen, the wire is rectangular in cross-section with a width of about 100 nm and a metal thickness of about 50 nm. The grating coupler is shown in Figure 9(b). This coupler is designed to first spread the plasmon mode, in the direction perpendicular to its propagation, and then deflect it to normal incidence with a grating.

---

[7] D. F. P. Pilea, T. Ogawa, D. K. Gramotnev, T. Okamoto, M. Haraguchi, M. Fukui, and S. Matsuo, "Theoretical and experimental investigation of strongly localized plasmons on triangular metal wedges for subwavelength waveguiding," *Applied Physics Letters*, vol. 87, pp. 061106, 2005.

[8] S. A. Maier, M. D. Friedman, P. E. Barclay, and O. Painter, "Experimental demonstration of fiber-accessible metal nanoparticle plasmon waveguides for planar energy guiding and sensing," *Applied Physics Letters*, vol. 86, pp. 071103, 2005; S. A. Maier, P. E. Barclay, T. J. Johnson, M. D. Friedman, and O. Painter, "Low- loss fiber accessible plasmon waveguide for planar energy guiding and sensing," *Applied Physics Letters*, vol. 84, pp. 3990, 2004.

[9] W. Nomuraa, M. Ohtsub, and T. Yatsui, "Nanodot coupler with a surface plasmon polariton condenser for optical far/near-field conversion," *Applied Physics Letters*, vol. 86, pp. 181108, 2005.

[10] L. Yin, V. K. Vlasko-Vlasov, J. Pearson, J. M. Hiller, J. Hua, U. Welp, D. E. Brown, and C. W. Kimball, "Subwavelength focusing and guiding of surface plasmons," *Nano Letters*, vol. 5, pp. 1399{1402, 2005.

[11] R. M. Dickson and L. A. Lyon, "Unidirectional plasmon propagation in metallic nanowires," *Journal of Physical Chemistry B*, vol. 104, pp. 6095{6098, 2000.

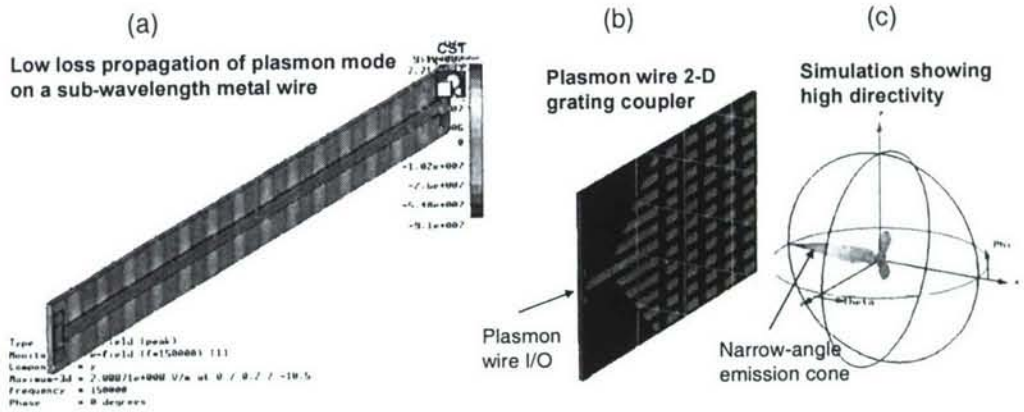

Figure 9. (a) FDTD simulation of the a rectangular plasmon wire showing low loss propagation, (b) Novel design for a plasmon wire normal-incidence coupler. In the propagation direction the grating elements are spaced by the plasmon wavelength, as expected. In the other direction, the optimum spacing is determined by simulation. (c) FDTD simulation showing the highly directive normal-incidence emission of the plasmon coupling structure.

Figure 10. Approaches attempted for fabrication of plasmon nanowires and couplers. Approach 1 consisted of the usual lift-off technique. In approach 2 the metal is deposited or grown on the whole wafer and the pattern is selectively etched. For approach 3 a metal mask is used to replace the PMMA in the lift-off technique. This allows higher temperature metal deposition.

The fabrication procedures attempted for these structures are shown in Figure 10. The first technique is the standard lift-off technique. Here the dielectric wafer is first coated with PMMA. This is exposed with a high-resolution e-beam lithography system and developed. Following this, metal is deposited on the whole sample. Unwanted metal is then removed by lifting off, or dissolving, the PMMA. The final step is a dielectric overcoat to match the refractive index of the base material. This approach is the simplest

in that it is standard. It also gave us high resolution as shown in the resist patterns in Figure 11(a and b). However, it tends to leave rough edges on the wires and these can scatter light. In practice, we found we could make good devices with this technique but the yield was sometimes low.

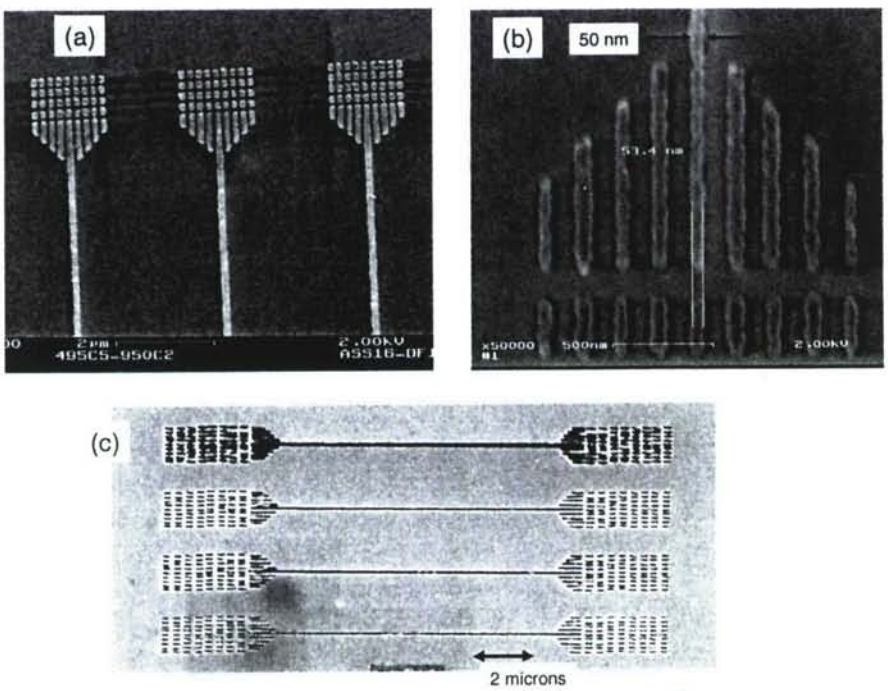

Figure 11. (a) Plasmon wire and coupling structure patterns in bi-layer PMMA. (b) Closeup of coupling structure showing 50 nm line widths. (c) FIB fabricated wires and couplers with large aspect ratios for different exposures. Lines as narrow as 30 nm were possible.

The second fabrication technique attempted was selective etching. Here a high quality, preferably single crystal metal film is first grown over the whole substrate. PMMA is then spun on, patterned with the e-beam and overcoated with a hard insulator. After lift off, the insulator covers the portions of the metal that are desired for the pattern. Next the unwanted metal is selectively etched by RIE, followed by the final dielectric overcoat. The advantage of this technique is that the edges will tend to be smooth and slightly rounded, instead of rough and ragged. Also, since there is no resist on the sample whenb the metal is deposited, this can be done at high temperature, ideally creating a single crystal metal layer, via lattice-matched growth. The problem we had with this technique was that the silver metal we used did not etch well. So the power was turned up, essentially sputtering it away. While this did remove the metal, the resolution was too low to make small structures.

The third fabrication technique attempted was to use a metal mask instead of PMMA resist. This has the advantage of allowing high temperature metal-film growth and patterning all in the same step. Here we expect high quality metal with smooth edges. The hard part of this technique is generation of the metal mask. This had to be done with a focused ion beam (FIB) by machining holes through a metal membrane. The

issues were stability of the metal film when making long wires with narrow width. Nonetheless our first attempts were encouraging, as shown in Figure 11(c).

Successfully fabricated nanowire and couplers, using the first method, are shown in Figure 12. These consisted of silver on MgF_2. Earlier we used a chromium wetting adhesion layer, but later discontinued this practice because of concerns about the potential for large losses in the chromium. As can be seen, large aspect ratios were possible. Wire lengths of 5, 10, 13, 14, 15 and 16μm microns were made. In this run, the wire cross section was 100nm x 50nm. In later runs, even smaller wires were made.

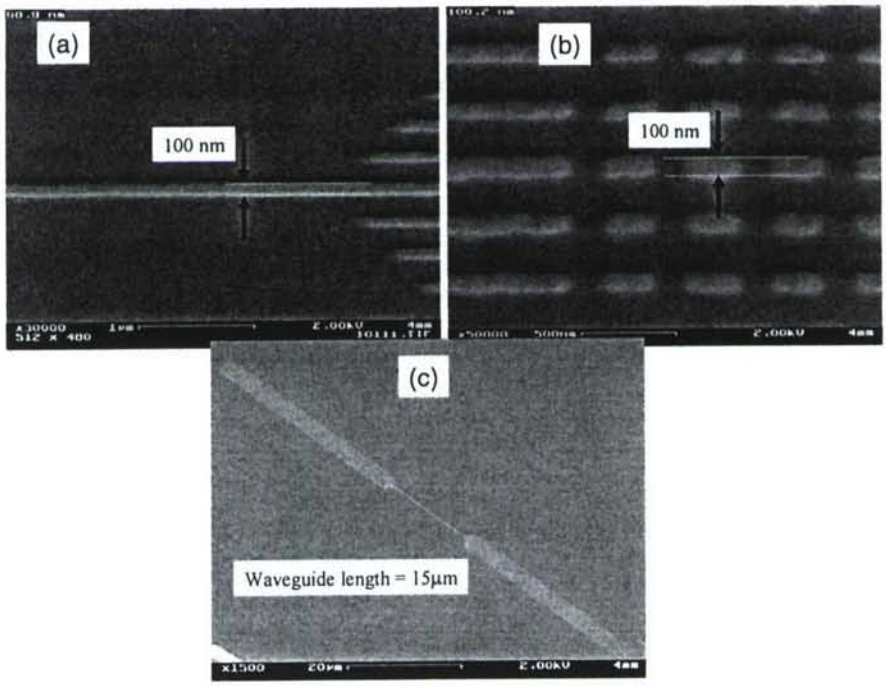

Figure 12. Silver on MgF2. (a) Narrow 100 nm wide plasmon nanowire. (b) 100 nm wide elements in coupling structure. (c) Long uninterrupted wire lengths.

The light transmission of a 5 micron wire with couplers is shown in Figure 13. The laser is input on the left and the output is clearly visible on the right. The images are reverse contrast for clarity. In this experiment, different parts of the input grating were illuminated. When the top part was illuminated, a bright output spot was seen only at the top of the output grating. A similar result appears for illumination of the bottom part of the input grating. When the center of the input grating is illuminated, no bright spot appears at the output but both top and bottom parts show light transmission. We take this behavior to be evidence that the light is localized to one edge of the 100 nm wide wire.

From the data in Figure 13 we estimate the coupling efficiency of the grating to the wire and back out again is about 0.3%. To determine this, we analyzed the image from the camera and integrated the total light on the output coupler. To avoid any error due to scattered light we repeated the experiment on an identical set of couplers that were fabricated without a nanowire, and subtracted the numbers. We then deduced the intensity of the input laser using attenuators until it showed comparable brightness on the camera, and integrated over the small sized laser spot. Based on the attenuators used we then calculated the total transmission of the structure.

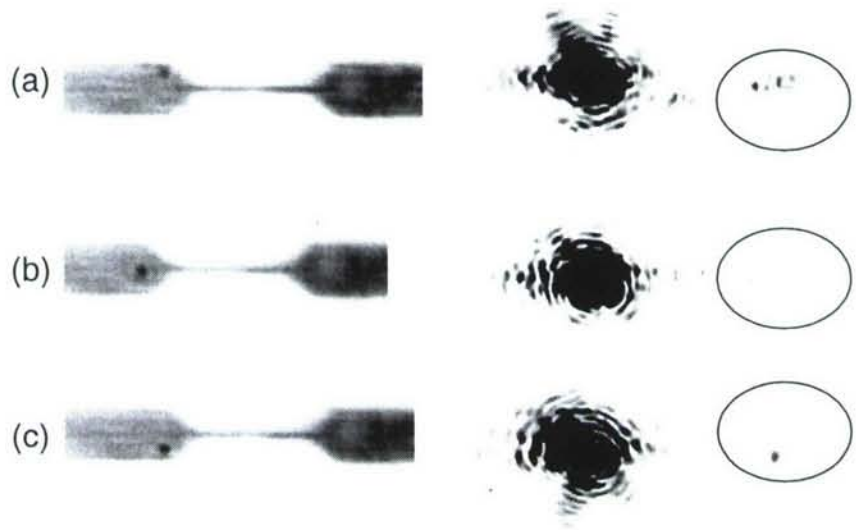

Figure 13. Light transmitted by nano-wire. The left column shows the white light image of the wire structure where the position of the input laser spot is seen as a small dark dot on the left grating structure. The right column shows the output from the coupler on the right. No white light is present. The circles are centered approximately on the output coupler. (a) shows illumination of the upper part of the input grating, (b) shows illumination of the center part and (c) shows illumination of the lower part.

To determine the transmission loss of the nanowires we then repeated this entire experiment for structures having different wire lengths, but identical coupling structures. The result showed about 0.5 dB/micron loss for the nano-wire. We achieved a similar result whether we used the integrated light intensity on the output coupler or the intensity of the brightest spot. This is significantly better than previous measurements made on small wires in the visible.

On the 50 nm wide wires we noticed a significant nonlinearity in the transmission losses. For lengths shorter than 13 microns we see an exceptionally low loss of 0.13 dB/microns. Beyond 13 microns of wire length the loss increases abruptly. Again we see similar results whether we use integrated or peak power at the output coupler. At the same time, when we do position selective illumination of the input grating as in Figure 13. We see that light remains on one side of the wire only for the 5 micron long wires. After 10 microns, both sides of the output coupler light up equally. In the case of the 100 nm wide wires, we do not see light crossover even for up to 15 micron wire lengths. We interpret these observations as indicating that the tightly confined mode can have very low loss, but is eventually mixing with other more-lossy modes for long wire lengths.

To estimate the input and output coupling efficiency of the grating, we analyzed the input and output spot patterns in detail. This is shown in Figure 14(a). As can be seen, a portion of the input light appears to be propagating in both directions at the input with the same fringe spacing as seen at the output coupler. By measuring the total propagating light intensity at the input, we conclude that the grating couples about 1% of the incident light into the in-plane propagating mode. Knowing the total input/output optical efficiency and the wire loss as a function of length, we then conclude that the output

coupler is about 35% efficient. This is relatively high considering that symmetry arguments allow at most half of the light to propagate toward the camera.

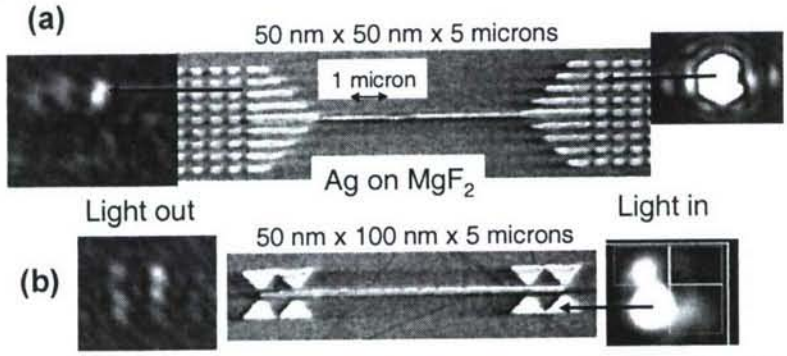

Figure 14. (a) Input and output spot patterns used to estimate coupling efficiencies of the grating couplers. Structures are silver on MgF_2 with MgF_2 overcoat to match refractive index of substrate. Length 5 microns, width 50 nm, height 50 nm. (b) Input/output coupling for bowtie antenna couplers. Here the wire is 100 nm wide.

We also investigated different input/output couplers. Figure 14(b) shows a 5 micron long optical wire with bowtie antenna couplers. In this example the wire is 100 nm wide. Here both sides of the wire are excited by the input laser as shown by the output pattern. To estimate efficiency we measured the coupling from the illuminated bowtie to the others. As seen in Figure 14(b), 7% of the input light focused on one bowtie antenna is coupled into an adjacent antenna, both on the same and opposite sides of the wire. However, it is not clear what the input and output coupling efficiencies to the wire are in this case. Looking at the output coupler, we find that both output antenna pairs out-couple equal light power, as seen in Figure 14(b). If significant optical power were coupled out by the first bowtie pair, then less should be out-coupled by the second, in analogy to the decay seen at the grating out-coupler in Figure 14(a). This implies that the bowties are less efficient as out-coupling devices than the gratings.

5. Summary

Although we were not able to duplicate the metallic fractal patterns due to e-beam resolution limitations, significant progress was made for other structures, and simulations show that one of these can meet our project goal of developing plasmon-based atom-photon couplers for quantum computing.

A microwave version of an infrared LC resonator with variable coupling was designed and tested. The test results agreed well with theory even in the near field. An IR version of this resonator was easily fabricated with e-beam lithography. This plasmon resonator structure should be suitable for incorporating in optical cavities to observe multiplicative field enhancement.

The results obtained for optical nano-wires are very significant. The propagation losses of 0.5 dB/micron match those of the best self-assembled wires in the case of 100 nm wide wires. For the 50 nm wires, the propagation losses are 5 times lower for wire lengths less than 10 microns, though they increase sharply for longer lengths. These low propagation losses are surprising because these wires were fabricated by e-beam deposition and lift-off, and therefore are not single crystal and probably have rough corners.

The output coupling efficiency of the grating coupler is very high (~35%). However the input coupling efficiency is low (~1%). The bowtie antenna couplers appear to have better in-coupling efficiency (~7%) but so far lower out-coupling efficiency.

Indirect evidence of strong mode confinement exists because light input on one side of the 100 nm wire stays on that side, even for propagation lengths longer than 10 microns. Theory shows that the confinement should be high enough to couple most of the light from an atom into the guided plasmon mode. This means that we can reach the goal of quantum high-fidelity quantum coupling between photons and atoms using only wires.